Article

Cell Stem Cell

Ascl2 Acts as an R-spondin/Wnt-Responsive Switch to Control Stemness in Intestinal Crypts

Graphical Abstract

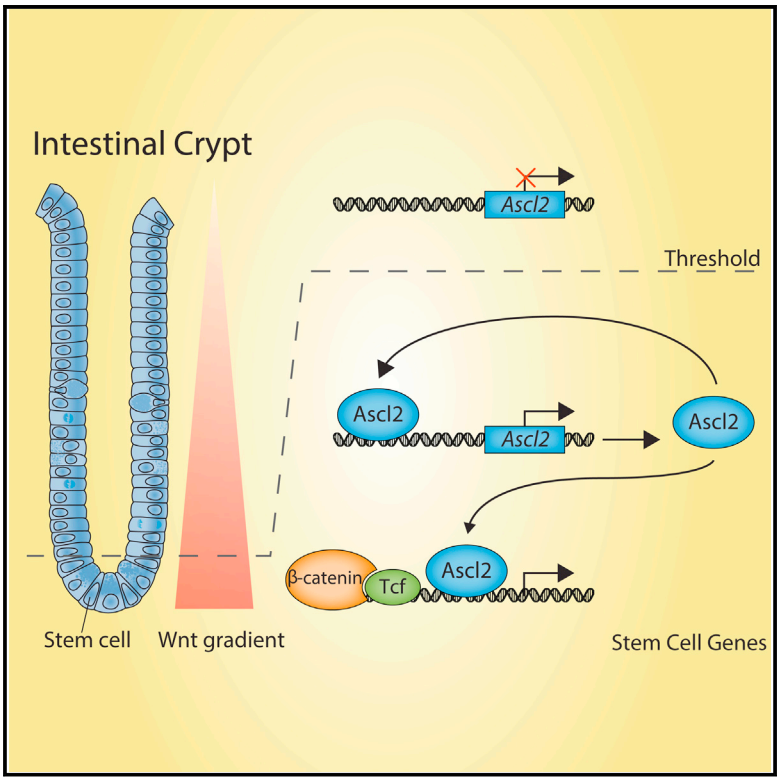

Authors

Jurian Schuijers, Jan Philipp Junker, ..., Alexander van Oudenaarden, Hans Clevers

Correspondence

h.clevers@hubrecht.eu

In Brief

The Wnt signaling pathway controls stem cell identity in the intestinal epithelium, but it has remained unclear how the continuous Wnt gradient is translated into discrete cell type specification. Schuijers et al. show that the transcription factor Ascl2 forms a bimodal switch that interprets Wnt levels and specifies stem cells.

Highlights

- Wnt and Ascl2 activate a gene signature fundamental to the intestinal stem cell state
- β-catenin/Tcf4 and Ascl2 co-occupy DNA and synergistically activate transcription
- Ascl2 forms an autoactivating loop that leads to an on/off expression pattern
- This loop translates the Wnt gradient into a discrete transcriptional decision

Accession Numbers

GSE57053

Schuijers et al., 2015, Cell Stem Cell *16*, 1–13
February 5, 2015
http://dx.doi.org/10.1016/j.stem.2014.12.006

CellPress

Please cite this article in press as: Schuijers et al., Ascl2 Acts as an R-spondin/Wnt-Responsive Switch to Control Stemness in Intestinal Crypts, Cell Stem Cell (2015), http://dx.doi.org/10.1016/j.stem.2014.12.006

Cell Stem Cell
Article

Ascl2 Acts as an R-spondin/Wnt-Responsive Switch to Control Stemness in Intestinal Crypts

Jurian Schuijers,[1] Jan Philipp Junker,[1] Michal Mokry,[2] Pantelis Hatzis,[3] Bon-Kyoung Koo,[1,4,5] Valentina Sasselli,[1] Laurens G. van der Flier,[1,6] Edwin Cuppen,[1] Alexander van Oudenaarden,[1] and Hans Clevers[1,*]
[1]Hubrecht Institute, Royal Netherlands Academy of Arts and Sciences (KNAW), University Medical Centre Utrecht, CancerGenomiCs.nl, Uppsalalaan 8, 3584 CT Utrecht, the Netherlands
[2]Department of Pediatric Gastroenterology, Wilhelmina Children's Hospital, University Medical Centre Utrecht, 3508 AB Utrecht, the Netherlands
[3]Biomedical Sciences Research Center "Alexander Fleming," 16672 Vari, Greece
[4]Wellcome Trust–Medical Research Council Stem Cell Institute, University of Cambridge, Tennis Court Road, Cambridge CB2 1QR, UK
[5]Department of Genetics, University of Cambridge, Downing Street, Cambridge CB2 3EH, UK
[6]SomantiX B.V., Utrecht, Padualaan 8, 3584 CH Utrecht, the Netherlands
*Correspondence: h.clevers@hubrecht.eu
http://dx.doi.org/10.1016/j.stem.2014.12.006

SUMMARY

The Wnt signaling pathway controls stem cell identity in the intestinal epithelium and in many other adult organs. The transcription factor Ascl2 (a Wnt target gene) is a master regulator of intestinal stem cell identity. It is unclear how the continuous Wnt gradient along the crypt axis is translated into discrete expression of Ascl2 and discrete specification of stem cells at crypt bottoms. We show that (1) Ascl2 is regulated in a direct autoactivatory loop, leading to a distinct on/off expression pattern, and (2) Wnt/R-spondin can activate this regulatory loop. This mechanism interprets the Wnt levels in the intestinal crypt and translates the continuous Wnt signal into a discrete Ascl2 "on" or "off" decision. In turn, Ascl2, together with β-catenin/Tcf, activates the genes fundamental to the stem cell state. In this manner, Ascl2 forms a transcriptional switch that is both Wnt responsive and Wnt dependent to define stem cell identity.

INTRODUCTION

Intestinal crypts contain Lgr5^{+} stem cells and their transit-amplifying (TA) daughter cells, as well as terminally differentiated Paneth cells. Cells exiting crypts terminally differentiate into enterocytes, goblet cells, M-cells, Tuft cells, and enteroendocrine cells and move up the flanks of the villi to undergo apoptosis upon reaching the villus tips (Clevers, 2013). Paneth cells escape the crypt-villus flow by migrating to crypt bottoms where they persist for several weeks (Bjerknes and Cheng, 1981). With the exception of stem cells and Paneth cells, the intestinal epithelium is renewed approximately every 5 days (Stevens and Leblond, 1947).

Proliferation of epithelial crypt cells is Wnt dependent. Thus, mice that are mutant for the intestine-specific member of the Tcf transcription factor family, *Tcf4*/*Tcf7l2*, fail to establish proliferative crypts during late gestation (Korinek et al., 1998), while conditional deletion of *β-catenin* (Fevr et al., 2007; Ireland et al., 2004) or *Tcf4* (van Es et al., 2012a), as well as transgenic expression of the secreted *Dickkopf-1* Wnt inhibitor (Kuhnert et al., 2004; Pinto et al., 2003), leads to disappearance of proliferative crypts in adult mice. Moreover, malignant transformation of intestinal epithelium is almost invariably initiated by activating Wnt pathway mutations (Korinek et al., 1997; Morin et al., 1997).

Detailed analysis of the Wnt-driven target gene program (as expressed in colon cancer cells and in crypts) has revealed that three main categories of target genes can be recognized (Van der Flier et al., 2007). First, target genes like *Axin2*, *cMyc*, *CD44*, and *cyclinD1* are expressed in all proliferative crypts cells, most obviously in the TA cells (Fevr et al., 2007; ten Kate et al., 1989). Second, genes like *MMP7* and *EphB3* and defensins/cryptdins (Batlle et al., 2002; Bevins and Salzman, 2011) are expressed specifically in the terminally differentiated Paneth cells, and, indeed, formation of Paneth cells is Wnt dependent (Andreu et al., 2005, 2008; Farin et al., 2012; van Es et al., 2005a). Third, target genes such as *Lgr5*, *Ascl2*, *Nr2E3*, and *Troy* (Itzkovitz et al., 2011; Muñoz et al., 2012) are restricted to crypt base columnar cells (CBC), originally postulated by Cheng and Leblond (1974) to represent the crypt stem cells, a notion confirmed by an Lgr5-based lineage tracing experiment (Barker et al., 2007).

Ascl2 (*Mash2*/*HASH2*) is homologous to the *Drosophila* Achaete-scute complex genes (Johnson et al., 1990). It encodes a basic helix-loop-helix (bHLH) transcription factor with an unusually restricted expression pattern. During development, its expression is predominantly detected in extraembryonic tissues (Guillemot et al., 1994). *Ascl2*$^{-/-}$ embryos die from placental failure around embryonic day (E)10.5 (Guillemot et al., 1994). In the adult, the gene is expressed in a Wnt-dependent and highly restricted fashion in intestinal stem cells (Itzkovitz et al., 2011; Jubb et al., 2006; Muñoz et al., 2012; Sansom et al., 2004 ; Van der Flier et al., 2007, 2009b), and it has recently been shown to initiate T-helper-cell development (Liu et al., 2014). Conditional knockout of *Ascl2* in the adult intestinal epithelium results

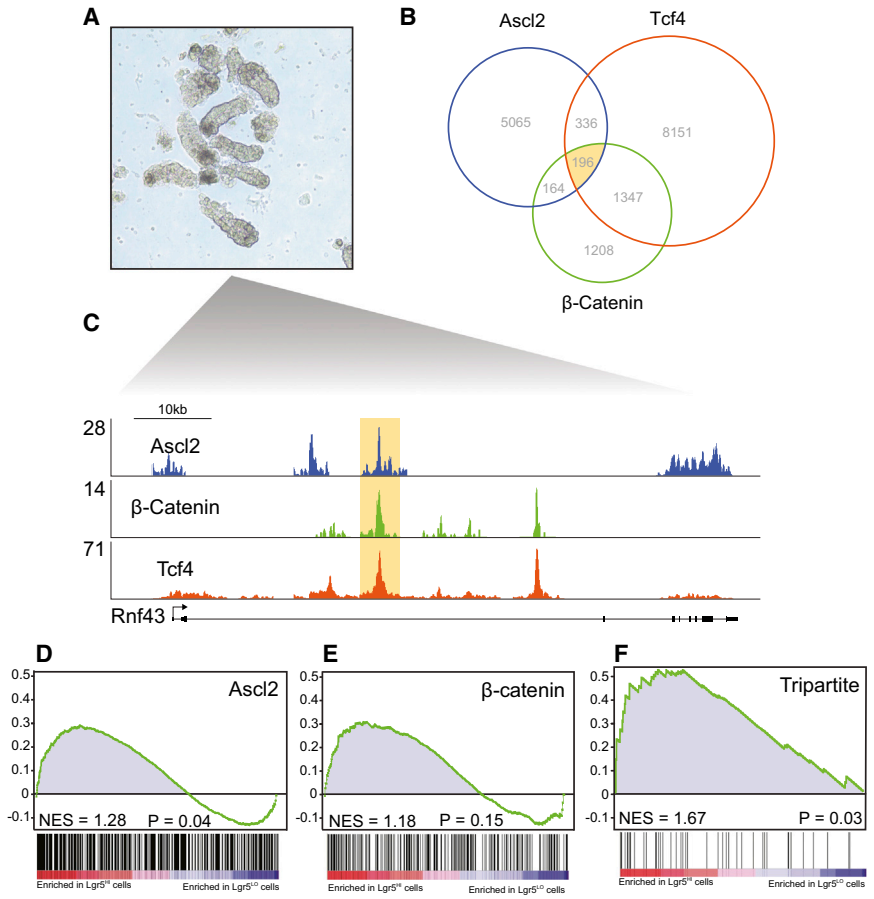

Figure 1. Ascl2 and β-Catenin/Tcf4 Co-occupy DNA Elements in Mouse Intestinal Crypts and Drive a Stem Cell Program

(A) Crypts were isolated from fresh intestines after removal of villi tissue by calcium washout with EDTA. This material was used to determine the binding patterns of Ascl2, β-catenin, and Tcf4 in the mouse intestine.

(B) Venn diagram showing the overlap of Ascl2, β-catenin, and Tcf4 binding sites. Peaks were called overlapping when at least 10 bp were simultaneously occupied in both peak sets.

(C) Example of the ChIP-Seq patterns of Ascl2, β-catenin, and Tcf4. The *Rnf43* locus is displayed.

(D–F) GSEA probing for enrichment of (D) Ascl2-associated, (B) β-catenin-associated, or (C) tripartite-peak-associated gene sets in $Lgr5^{HI}$ stem cells versus $Lgr5^{LO}$ cell expression analysis. Gene sets exist of genes with a ChIP-seq peak within 5 kb of their TSS. The used gene list was obtained from a comparison of the gene expression from sorted $Lgr5^{HI}$ versus $Lgr5^{LO}$ daughter cells. Red indicates genes enriched in $Lgr5^{HI}$ stem cells. Blue indicates genes enriched in $Lgr5^{LO}$ daughter cells.

See also Figure S1.

in the rapid replacement of the mutant cells by wild-type *Ascl2*$^{+/+}$ escaper stem cells. Conversely, ectopic expression of *Ascl2* using the intestinal epithelium-specific *Villin* promoter (Pinto et al., 1999) induces hyperproliferation of crypts, expansion of the expression domain of the stem cell markers *Lgr5* and *Sox9*, and the formation of hyperproliferative pockets on the villus (van der Flier et al., 2009b). This has led to the conclusion that *Ascl2* is a master regulator of crypt stemness. Nevertheless, *Ascl2* is not an oncogene, as overexpression in the APC^{min} background does not lead to elevated tumor initiation or progression (Reed et al., 2012). Here, we investigate how the Wnt target gene *Ascl2* cooperates with the generic Wnt effector β-catenin/Tcf4 to control the stem-cell-specific subset of intestinal Wnt target genes and, thus, to regulate stemness in the intestinal epithelium.

RESULTS

Tcf4/β-Catenin and Ascl2 Co-occupy DNA and Drive a Stem Cell Program

To investigate the mechanism through which Ascl2 controls its target genes, we surveyed Ascl2 DNA binding in isolated murine intestinal crypts yielding 5,761 high-confidence binding sites (Figures 1A–1C; Table S1). We then identified the genes that are potentially regulated by Ascl2. We assigned genes to Ascl2-occupied elements based on the distance of the element to the transcriptional start site (TSS) of an annotated gene. The accumulated binding pattern of assayed transcription factors (TFs) relative to all TSSs showed a local maximum within 5 kilobases (kb) (Figure S1A); thus, this distance was used as a cutoff. Using the RefSeq database, we scored genes with an occupancy peak within 5 kb of the TSS. This resulted in a TF-associated gene set consisting of 679 genes. The signature gene set was then correlated to the gene list obtained from comparing isolated intestinal $Lgr5^{+}$ stem cells to their closest relatives, the immediate TA daughter cells (Muñoz et al., 2012), using a gene set enrichment analysis (GSEA) (Mootha et al., 2003; Subramanian et al., 2005) (Figure 1D) and found a significant enrichment of Ascl2 target genes with the stem cell signature (normalized enrichment score [NES] = 1.28).

The intestinal epithelium is known to be strictly dependent on Wnt signals for its homeostatic proliferation, as removal of Wnt components (Korinek et al., 1998; van Es et al., 2012a) or introduction of Wnt inhibitors (Pinto et al., 2003; Kuhnert et al., 2004) abrogates this proliferation. Therefore, we also performed chromatin immunoprecipitation sequencing (ChIP-seq) for Wnt pathway components Tcf4 and β-catenin (Schuijers et al., 2014) (Table S1). When comparing the data sets, of the 5,761 Ascl2 binding events, 9% overlapped with the 10,030 Tcf4 binding sites. β-catenin ChIP-seq yielded 2,915 binding events, of which almost 53% overlapped with Tcf4. A total of 196 elements were found to be occupied by all three factors, further referred to as "tripartite elements" (Figure 1B). On tripartite elements, the components for active Wnt signaling and Ascl2-driven activation converge.

In a GSEA, β-catenin-associated genes were slightly enriched in stem cells, but genes with tripartite elements were more enriched in the stem cells than were genes occupied by Ascl2 or

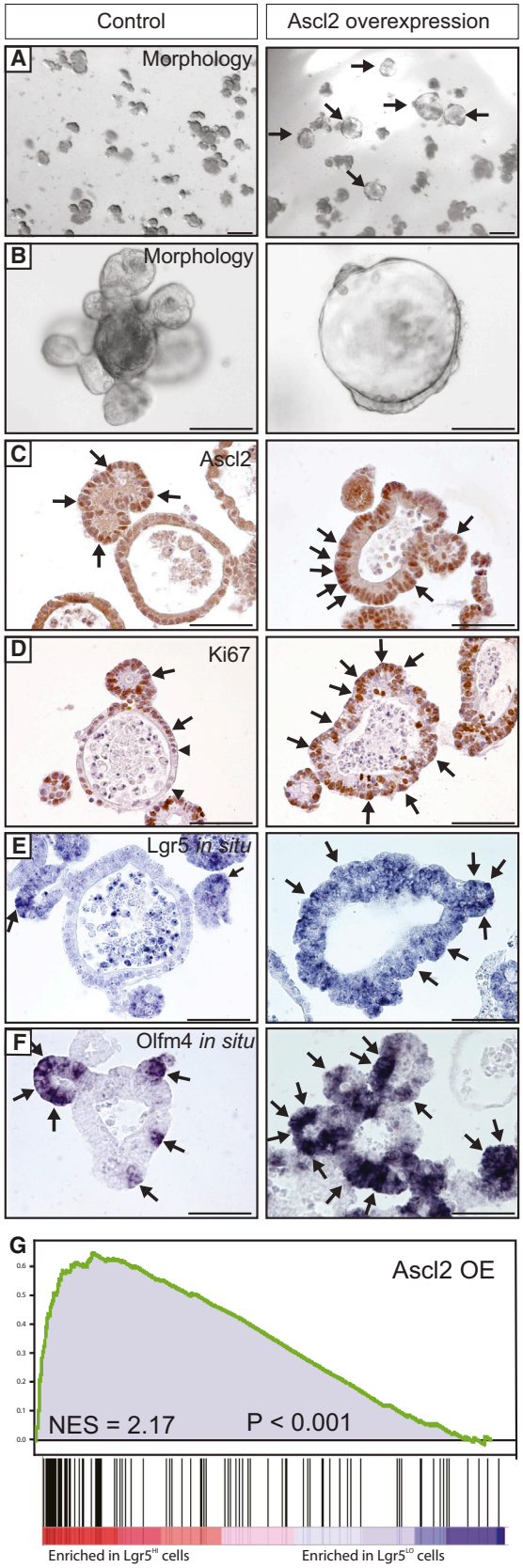

Figure 2. β-Catenin/Tcf4 and Ascl2 Cooperatively Activate a Stem Cell Transcriptional Program in Organoids

(A and B) Organoids expressing Ascl2 adapt a cyst-like morphology similar to that of Wnt-treated organoids. Phase contrast microscopy shows the change in morphology upon Ascl2 overexpression.

(C–F) Histology showing increased expression of (C) Ascl2 (arrows), (D) activation of Ki67 (arrows), and in situ hybridization showing upregulation of the stem cell markers (E) *Lgr5* (arrows) and (F) *Olfm4* (arrows).

(G) GSEA probing for enrichment of Ascl2-induced genes in $Lgr5^{HI}$ stem cell versus $Lgr5^{LO}$ daughter cell expression analysis. Gene sets consist of genes that are >1.5-fold upregulated upon overexpression of Ascl2 in organoids. Red indicates genes enriched in $Lgr5^{HI}$ stem cells. Blue indicates genes enriched in $Lgr5^{LO}$ daughter cells.

Scale bars, 100 μm.

β-catenin alone: NES = 1.18 (β-catenin), 1.67 (tripartite) (Figures 1E and 1F). Tcf4-occupied genes were expressed in stem cells as well as daughter cells and did not correlate significantly with either cell type. We conclude that tripartite occupancy is a strong indicator for genes of the stem cell program in the intestinal epithelium.

Ascl2 Induces the Formation of Stem Cells In Vitro

We studied the ability of Ascl2 to induce the expression of stem cell genes into cultured mouse miniguts, expanding epithelial organoids that preserve the in vivo kinetics and cell type distribution of crypts and villi (Sato et al., 2009). Using a retroviral infection protocol (Koo et al., 2011), we introduced *Ascl2* under control of a lox-stop-lox cassette into mouse *Villin-creERT2* (Pinto et al., 1999) organoids. Upon 4-hydroxytamoxifen (4-OHT) stimulation and the consequent expression of Ascl2 (Figure 2C), the organoids changed their morphology (Figures 2A and 2B). Ascl2-expressing organoids lost their propensity to bud and displayed cystic morphology resembling wild-type organoids grown under exogenous Wnt3a (Farin et al., 2012) (Figure 2B). Further analysis of these organoids revealed Ascl2 expression in all cells of the organoids and an increased amount of Ki67-positive cycling cells, as well as increased numbers of cells expressing the stem cell markers *Lgr5* and *Olfm4* (Figures 2D–2F). A total of 216 genes were significantly upregulated (≥1.5-fold) 1 day after induction, as determined by microarray analysis, including the stem cell markers *Lgr5*, *Smoc2* (Muñoz et al., 2012), and *Ephb2* (de Sousa E Melo et al., 2011; Jung et al., 2011; Muñoz et al., 2012). This gene set showed a strong correlation with the gene list obtained from comparing isolated intestinal $Lgr5^{+}$ stem cells with their immediate daughter cells (Figure 2G) (Muñoz et al., 2012). These observations confirmed the notion that Ascl2 controls the stem cell state (van der Flier et al., 2009b) and validated the minigut approach as an assay for Ascl2 function.

Ascl2 and Tcf4 Converge Transcriptionally in Cultured Small Intestinal Organoids

To investigate whether Ascl2 and β-catenin/Tcf4 cooperate in maintaining stem cells, mice containing the $Ascl2^{loxp/loxp}$ allele (van der Flier et al., 2009b) were crossed with *VillinCreERT2* mice. Organoids were derived from F1 animals, and the Ascl2 gene was deleted with a pulse of 4-OHT in vitro. Ascl2-deficient organoids survived the removal of Ascl2 yet underwent a change in morphology. They contained narrow crypts with, on average,

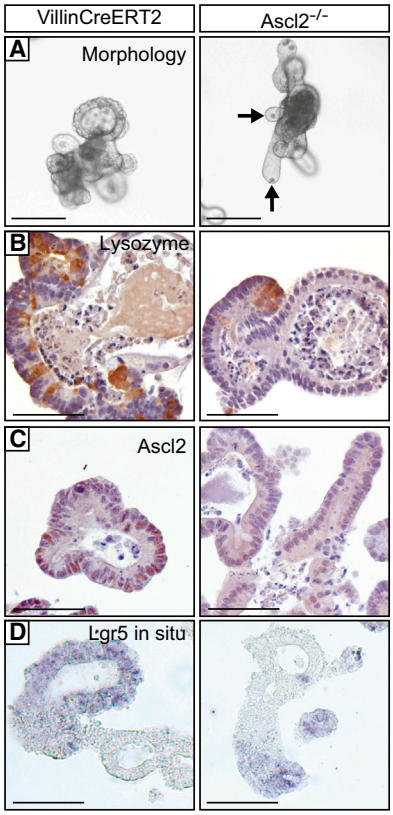

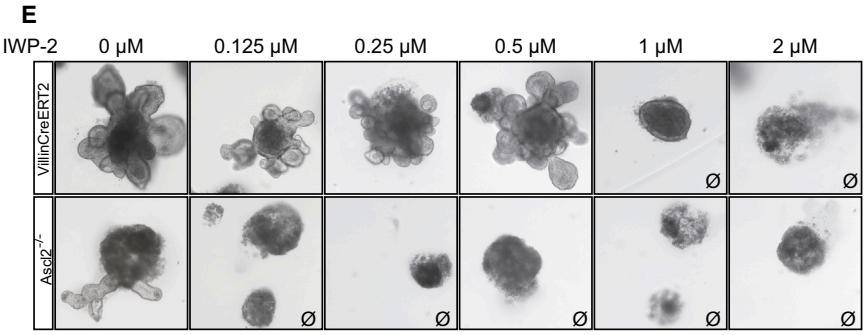

Figure 3. *Ascl2*$^{-/-}$ Organoids Have Altered Morphology and Are More Sensitive to Wnt Withdrawal

(A) Bright-field image of *Ascl2*$^{-/-}$ organoids showing narrow crypts supporting limited numbers of Paneth cells (arrows).

(B) Immunohistochemistry showing a decrease in the number of lysozyme-positive Paneth cells in *Ascl2*$^{-/-}$ organoids.

(C) Immunohistochemistry showing the complete loss of Ascl2 in *Ascl2*$^{-/-}$ organoids.

(D) In situ hybridization showing the continued expression of *Lgr5* in *Ascl2*$^{-/-}$ organoids.

(E) Bright-field images showing the increased sensitivity of *Ascl2*$^{-/-}$ organoids to the porcupine inhibitor IWP-2. Wild-type and *Ascl2*$^{-/-}$ organoids were grown in normal culture medium or in medium containing increasing concentrations of the porcupine inhibitor IWP-2.

Scale bars, 100 μm. Ø, organoids no longer viable. See also Figure S1.

~2.5-fold lower numbers of Paneth cells (Figure S1B), indicating a change in Wnt-dependent Paneth cell differentiation in these organoids (Figures 3A and 3B). Additionally, Ascl2-deficient organoids proliferated at approximately 33% of the speed of control organoids based on splitting ratios required to maintain equivalent culture density. Histology confirmed loss of Ascl2, but in situ hybridization showed that the expression of the stem cell marker *Lgr5* in the remaining stem cells was unchanged (Figures 3C and 3D). In order to give a more quantitative measure of the part of the stem cell signature that is directly influenced by Ascl2, we used the previously published stem cell signature containing 510 genes (Muñoz et al., 2012). Of these 510 genes, 138 are downregulated (1.5-fold) when Ascl2 is deleted (27%). This overlap represents the fraction of stem cell genes that are directly under control of Ascl2, since Ascl2-deficient organoids still contain Lgr5^{+} stem cells (Figure 3D). We concluded that simultaneous removal of Ascl2 in all the stem cells of the organoid system reduces growth but allows the survival of cycling Lgr5^{+} stem cells. The morphology of the Ascl2-deficient organoids was reminiscent of that of Wnt3-deficient organoids previously generated in our lab (Paneth cell-produced Wnt3 being the only source of Wnt in culture) (Farin et al., 2012). In these organoids, Wnt-dependent generation of Paneth cells is abolished, and stem cell growth is no longer supported. In order to test the putative link between Ascl2 and Wnt, we added IWP-2 to the organoid cultures in increasing amounts. IWP-2 inactivates porcupine, thereby inhibiting the palmitoylation and secretion of Wnts from the "sending" cell, which, in miniguts, is the Paneth cell. While control organoids were able to survive in the presence of up to 1 μM IWP-2, Ascl2-deficient organoids died when exposed to as little as 0.125 μM IWP-2 (Figure 3E). When high-dose IWP-2 is given to mice (Kabiri et al., 2014), or when the Porcupine gene (*Porcn*) is disrupted genetically (San Roman et al., 2014), Lgr5^{+} stem cells in the intestine disappear, and mice become moribund within 6 days. To see if this phenotype is confirmed in organoids, we treated wild-type organoids with different concentrations of IWP-2 inhibitor for 24 hr and tested Wnt target genes that are considered stem cell markers, *Lgr5* and *Rnf43*, as well as Wnt target genes that are not in the stem cell signature: *Aqp1* and *Cbx6*. As shown in Figure S1C, Wnt targets in the stem cells are more responsive to inhibition of the Wnt pathway by IWP-2 than other Wnt targets. We concluded that loss of Ascl2 leaves the organoids more dependent on Wnt signals for survival.

To assess if β-catenin/Tcf4 and Ascl2 cooperate to drive stemness, we sought to determine whether Ascl2-driven transcription can compensate for the loss of Wnt/Tcf4 signaling. Organoid

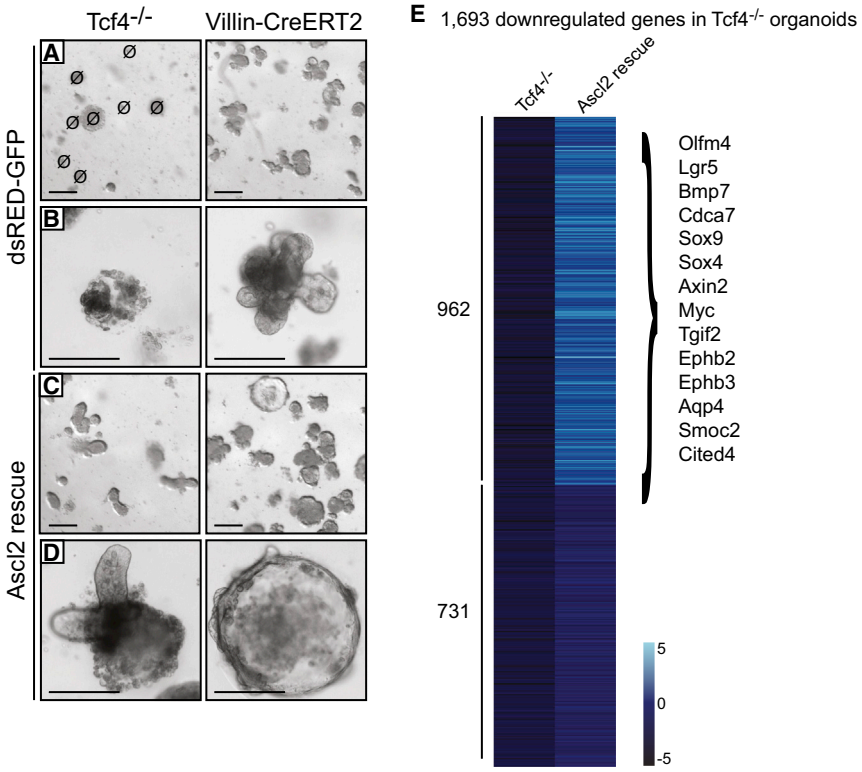

Figure 4. Ascl2 Overexpression Rescues *Tcf4*$^{-/-}$ Organoids by Activating Stemness Genes

(A–D) Survival of *Tcf4*$^{-/-}$ organoids upon Ascl2 expression. Phase contrast microscopy showing organoids derived from *VillinCreERT2;Tcf7l2*$^{loxp/loxp}$ and *villinCreERT2* animals that have been induced by a pulse of 4-OHT in vitro to recombine the floxed *Tcf4* allele. In (A) and (B), these organoids were transduced with a mock control retrovirus, and *Tcf4*$^{-/-}$ organoids do not survive (Ø). In (C) and (D), these organoids were transduced with a retrovirus carrying *Ascl2* cDNA under control of a floxed roadblock open reading frame. A pulse of 4-OHT that deletes *Tcf4* also induces the expression of *Ascl2*. *Ascl2*-overexpressing *Tcf4*$^{-/-}$ organoids survive, and *Ascl2*-overexpressing *VillinCreERT2* control organoids change morphology to grow in a cyst. Scale bars, 100 μm.

(E) Heat map showing the 962 rescued genes out of the 1,693 genes that are downregulated upon *Tcf4* knockout. Microarray was performed using mRNA isolated from organoids that had deleted *Tcf4* or had deleted *Tcf4* while overexpressing *Ascl2*. Fold change is indicated by blue, maximum 5-fold up- or downregulated (see color bar). A selection of typical stem cell genes that are rescued is depicted next to the heat map.

See also Figure S2.

cultures were derived from the *VillinCreERT2;Tcf7l2*$^{loxp/loxp}$ mouse model (van Es et al., 2012a). Upon the addition of 4-OHT, these organoids excised exon 11 of *Tcf4*/*Tcf7l2*, coding for the majority of its highly conserved DNA binding domain. In vivo deletion of *Tcf4* in the crypts of the small intestine induces apoptosis within 36 hr, abolishes proliferating crypts, and leads to death of the animals at 9 days after induction, when the intestines almost completely lack crypts and villi (van Es et al., 2012a). In vitro, the *Tcf4*$^{-/-}$ organoids could be cultured for no more than 7 days when they had halted proliferation and eventually disintegrated (Figures 4A and 4B).

When Ascl2 expression was induced in organoids carrying VillinCreERT2 and *Tcf7l2*$^{loxp/loxp}$ alleles, these were rescued from lethality (Figures 4C and 4D). We have been able to passage rescued organoids for more than 3 months while maintaining normal morphology. However, Tcf4-mutant, Ascl2-overexpressing organoids proliferated at approximately half the rate of control organoids based on splitting ratios required to maintain equivalent culture density. Microarray analysis after *Tcf4* deletion revealed 1,693 genes to be significantly downregulated (≥1.5-fold; Figure 4E). This gene set included the stem cell markers *Lgr5*, *Olfm4*, and *Smoc2*, as well as classical Wnt targets like *CD44*, *Axin2*, and *Sox9*. When *Ascl2* was introduced, 58% (962) of these genes were rescued (≥1.5-fold upregulation; Figure 4E). The rescued gene set strongly correlated with the Lgr5^{+} signature gene set (Figure S2A) and contained 33% (170/510) of the published stem cell signature genes (Muñoz et al., 2012). To see if Ascl2-driven rescue of stem cell genes might be achieved through alternative TCF/LEF family members, we performed quantitative PCRs (qPCRs) probing for these members on freshly isolated organoid RNA. We were able to detect minimal levels of *Lef1* and *Tcf1* in addition to significant levels of Tcf4 (Table S2), indicating that such a mechanism might be possible. In conclusion, high levels of Ascl2 are able to compensate for the loss of Tcf4 signaling in organoids, reactivating a subset of Wnt-target genes and rescuing Tcf4$^{-/-}$ organoids from lethality.

Ascl2 and Tcf4/β-Catenin Synergistically Activate Transcription

Ascl2 and Tcf4/β-catenin converge transcriptionally and maintain stem cells in the intestinal epithelium. However, it is unclear what the function of this convergence is. Therefore, we next sought to investigate if co-occupied elements confer increased transcriptional output to the stem cell genes they regulate. We performed ChIP-seq in LS174T colorectal cancer cells yielding 8,595 ASCL2, 8,856 TCF4, and 2,238 β-catenin high-confidence binding sites, as well as the consensus E-box motif for ASCL2 binding (Figures S3A–S3C) (Schuijers et al., 2014). We identified 641 binding sites to be co-occupied by all three factors and tested several co-occupied DNA elements in a luciferase reporter assay in human embryonic kidney 293T (HEK293T) cells. These cells carry an intact Wnt pathway that is inactive in the absence of Wnt ligand, and they do not express ASCL2. To activate TCF4-driven transcription, a dominant-positive mutant of β-catenin (S33Y-β-catenin) was transfected (Morin et al., 1997; Polakis, 1999). To activate ASCL2-driven transcription, we used a hemagglutinin (HA)-tagged form of ASCL2 (Figure 5A). Forty-two percent (5 out of 12) of the tested reporters, among which are *SOX9*, *MYB*, and *NR2E3* enhancers, showed a small level of activation when co-transfected with either factor alone but a further activation

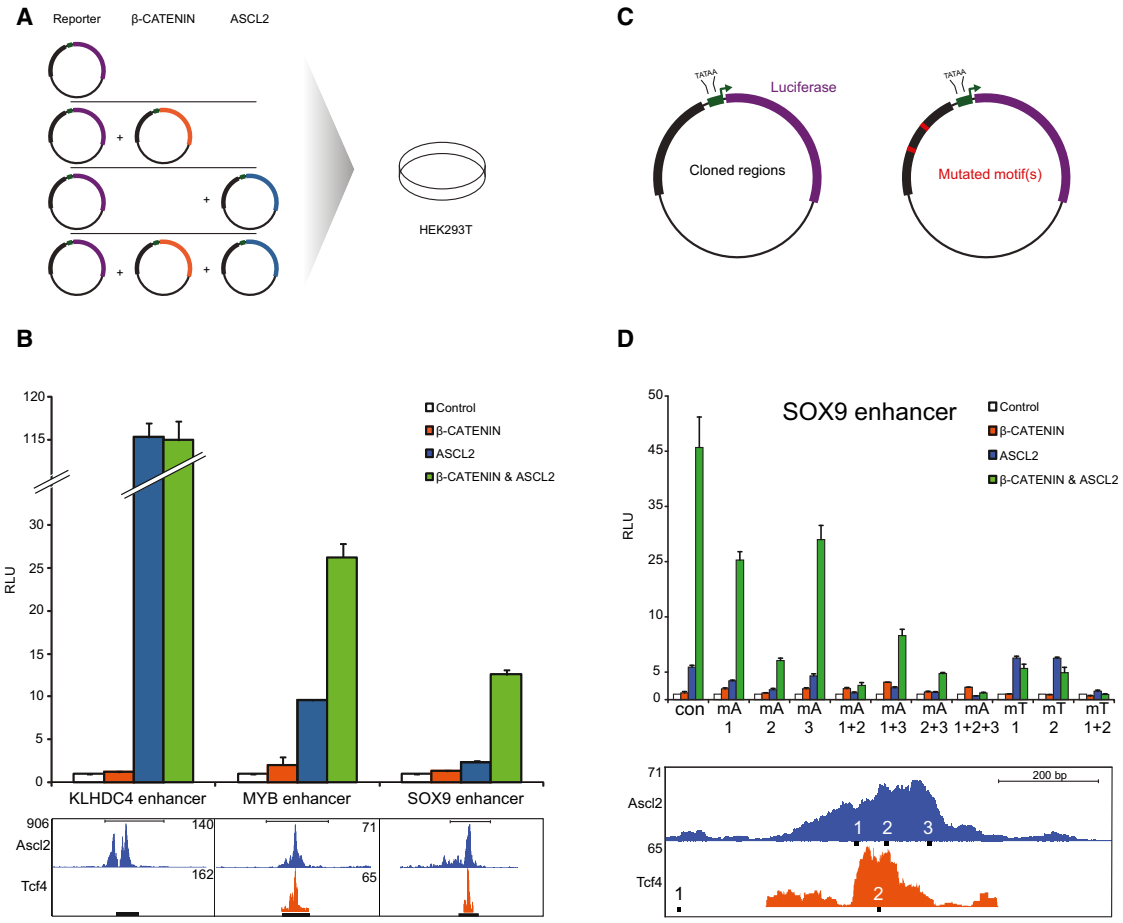

Figure 5. ASCL2 and β-Catenin/TCF4 Cooperatively Activate Target Genes

(A) Reporter plasmids were cotransfected with plasmids carrying either *β-catenin* or *Ascl2*, or with both plasmids. Mutation analysis was performed by introducing mutations to the DNA of the element in the reporter vector.

(B) Luciferase reporter assay in HEK293T cells showing synergistic activation by β-catenin/TCF4 and ASCL2 through specific enhancers. RLU, relative luciferase units. Luciferase activity was normalized with the value obtained from the pGL4.10 backbone without enhancer. ChIP-seq profiles with cloned elements (black bars) are depicted below. Scale bars, 1 kb. Triplicates of a representative experiment are shown. Error bars represent SD.

(C and D) Luciferase reporter assay in HEK293T cells showing loss of transcriptional activation of the SOX9 enhancer upon mutagenesis of ASCL2 or TCF4 motifs. The location of the mutated motifs and the ChIP-seq pattern over the cloned enhancers are shown in the bottom panel in (D) (numbers). con, the unaltered SOX9; mA, mutated ASCL2; mT, mutated Tcf4. Black bar indicates the cloned region. Luciferase activity was normalized with the value obtained from the pGL4.10 backbone without enhancer. Triplicates of a representative experiment are shown. Error bars indicate SD.

See also Figures S3 and S4.

when both ASCL2 and β-catenin were present (Figure 5B; Figure S3D). In contrast, elements that bound ASCL2 only were activated by ASCL2 and showed no further activation upon cotransfection with β-catenin (*KLHDC4*; Figure 5B). Conversely, the synthetic Wnt reporter TOP10, containing ten optimal TCF sites but no ASCL2 sites (van de Wetering et al., 1997), showed strong activation in response to S33-β-catenin (639-fold) but none upon transfection of ASCL2 alone and no additional activation when the two factors were cotransfected (Figure S3E). These results showed that concomitant binding of β-catenin/TCF4 and ASCL2 to certain DNA elements synergistically activates transcription.

To confirm these findings, we mutated all ASCL2 and TCF4 sites in two of the co-occupied elements. Removal of the majority of ASCL2 motifs in the SOX9 enhancer abolished ASCL2-induced activation, as well as the synergistic activation upon cotransfection of both factors, but did not change β-catenin-induced activation (Figures 5C and 5D). Conversely, mutation of the TCF4 motifs diminished β-catenin-induced activation and synergistic activation but left ASCL2-induced activation intact. However, mutation of both TCF4 sites resulted in a completely insensitive reporter. Mutational analysis of the MYB enhancer yielded similar results, with the exception that, here, removal of ASCL2 motifs also diminished the activation upon β-catenin cotransfection (Figure S4A). It is interesting that mutation of the binding motif of one factor reduced the ability of the enhancer to respond to the other factor. We conclude that the observed ability to synergistically activate transcription is dependent on the recruitment of both factors to their specific DNA motifs.

Ascl2 Forms a Bistable Switch

Ascl2 has been identified as a direct Wnt target in intestinal cell lines (Hatzis et al., 2008; Van der Flier et al., 2007) and, using ChIP-seq for Ascl2, we also observed a clear signal over the Ascl2 locus (Figure 6B). Thus, we hypothesized the existence of a feedback loop in which Ascl2 is capable of self-activation. This loop would be activated when a threshold level of Wnt activation would be reached to supply the initial amount of Ascl2, allowing two stable states that correspond to a stem-cell state (Ascl2-ON) and a non-stem-cell state (Ascl2-OFF) (Figure 6A). Ascl2 autoactivation would confer stability to this cell state and would allow a binary interpretation of the Wnt signal gradient that has been observed in the crypts of the intestine (Davies et al., 2008; Hirata et al., 2013).

We used single-molecule fluorescent in situ hybridization (smFISH) to test the putative autoactivation of Ascl2. This technique uses up to 96 oligonucleotides that are complementary to the coding sequence of the gene of interest and labeled with a single fluorophore each. Upon hybridization, individual mRNA molecules can be detected by fluorescence microscopy as diffraction-limited spots and quantified using computational methods (Itzkovitz et al., 2011; Raj et al., 2008). Stem cells in the tips of the buds of organoids cultured under normal conditions express clearly detectable levels of *Lgr5* and *Ascl2* (Figure 6C), with each dot representing an individual mRNA molecule. R-spondin1 is an obligatory medium constituent for minigut culture (Sato et al., 2009). It is a ligand for Lgr4 and Lgr5 and amplifies the Wnt signal in cells that express these receptors (Carmon et al., 2011; de Lau et al., 2011; Glinka et al., 2011; Hao et al., 2012; Koo et al., 2012). The source of R-spondins in the intestine is still poorly characterized, but several studies have indicated the stromal cells as a source for R-spondin2 and -3 (Kabiri et al., 2014; Wu et al., 2014), while the epithelium has been excluded as a source (Sato et al., 2009). When we reduced Wnt signal strength by removing R-spondin1 from the medium, we observed a strong decrease in the number of *Ascl2* mRNA molecules after as little as 3 hr (Figure S4B). This confirmed *Ascl2* as a direct Wnt target. After removal of R-spondin1 for 16 hr, low levels of *Lgr5* mRNA still persisted, while *Ascl2* mRNA was completely lost (Figure 6C). By using these remaining *Lgr5* transcripts as an identifier of stem cells, we could exclude all other cell types from our analysis.

To test if *Ascl2* expression was indeed regulated by an autoactivation loop, we titrated R-spondin1 into the culture medium of organoids that were either deprived of or contained normal amounts of R-spondin1 in the culture medium for 16 hr prior to the experiment. After 16 hr, we measured the number of *Ascl2* mRNA molecules in Lgr5$^+$ stem cells (Figure 6D). Thus, we observed a steep increase of *Ascl2* mRNA levels when titrating the amount of R-spondin1 (Figure 6E). Cells that had been cultured under normal R-spondin1 levels prior to the experiment showed a high level of *Ascl2* transcript density when they were exposed to medium containing as little as 1% of the R-spondin1 conditioned medium (CM) ("on state"). However, when they were cultured in medium containing less than 1% of R-spondin1 CM, *Ascl2* mRNA levels were reduced to a minimal "off state." This indicated that *Ascl2* is expressed in a bimodal fashion, switching between on and off states. Cells that had been cultured in the absence of R-spondin1 CM before the experiment also displayed *Ascl2* expression in an "on/off" pattern. However, the threshold level of R-spondin CM required to achieve "on-state" levels of *Ascl2* mRNA was increased to 1.75% R-spondin CM (Figure 6E). The ability of a biological system to respond not only to the current condition but also to a past condition is called hysteresis. The observed hysteretic activation of *Ascl2* expression in response to R-spondin levels is characteristic of an autoactivatory loop governing *Ascl2* expression (Acar et al., 2008; Ozbudak et al., 2004; Xiong and Ferrell, 2003) and could allow *Ascl2* expression to persist more robustly in a particular state upon fluctuation of the exogenous signal. In order to exclude the possibility that the hysteretic behavior of *Ascl2* expression is caused by a general mechanism in the Wnt pathway rather than autoactivation of *Ascl2*, we performed smFISH for a Wnt target that cannot autoactivate and is not activated by *Ascl2* expression. *Cbx6* is part of the polycomb repressor complex (Ogawa et al., 2002). It was downregulated in the absence of Tcf4 in our organoid system and did not contain detectable levels of Ascl2 ChIP-seq signal. We performed smFISH for *Cbx6* in the same R-spondin addition/withdrawal setup as before and saw a more gradual reduction of *Cbx6* transcript levels with lower R-spondin1 concentrations, confirming *Cbx6* as a Wnt target gene (Figures S5A and S5B). Notably, no hysteresis was observed, implying that the hysteretic behavior of *Ascl2* is not caused through Wnt pathway regulation.

We concluded (1) that *Ascl2* is regulated in a direct autoactivatory loop leading to a distinct on/off expression pattern of Ascl2 with a threshold that depends on the previous state and (2) that Wnt/R-spondin can activate this regulatory loop. This mechanism interprets the Wnt levels and gradients in the intestinal crypt and translates this continuous signal in a discrete Ascl2 "on" or "off" decision. In turn Ascl2, together with β-catenin/Tcf, activates the genes fundamental to the stem cell state. In this manner, Ascl2 forms a transcriptional switch that is both Wnt responsive and Wnt dependent to define stem cell identity.

DISCUSSION

As first shown in intestinal crypts (Korinek et al., 1998), Wnt signals are among the most prominent driving forces of adult stem cells (Clevers, 2013). The intestinal crypt is, arguably, still the best understood of Wnt-dependent adult stem cell niches. In crypts, Wnt signals are absolutely required for the maintenance of stem cells but also of proliferation of the TA cells and the generation of terminally differentiated Paneth cells. The distinction of the signal requirements of stem and TA cells on the one hand and Paneth cells on the other appears simple: stem and TA cells require Wnt and Notch signals, while inhibition of Notch signals in the presence of Wnt signals drives stem and progenitor cells toward a Paneth cell fate (Yin et al., 2014). It has been less clear what signals control the Lgr5$^+$ CBC stem cell phenotype versus that of TA cells, as both require Wnt, epidermal growth factor (EGF), and Notch signals and the absence of BMP signals (Fevr et al., 2007; Haramis et al., 2004; Sato et al., 2009; van Es et al., 2012a, 2005b). However, Lgr5$^+$ CBC cells are clearly distinct from their undifferentiated TA daughter cells. CBC cells are slender with a high nuclear versus cytoplasmic ratio and exhibit a cell cycle time of approximately 24 hr, while TA cells cycle every 12 hr. Moreover, Lgr5$^+$ CBC cells express a set of

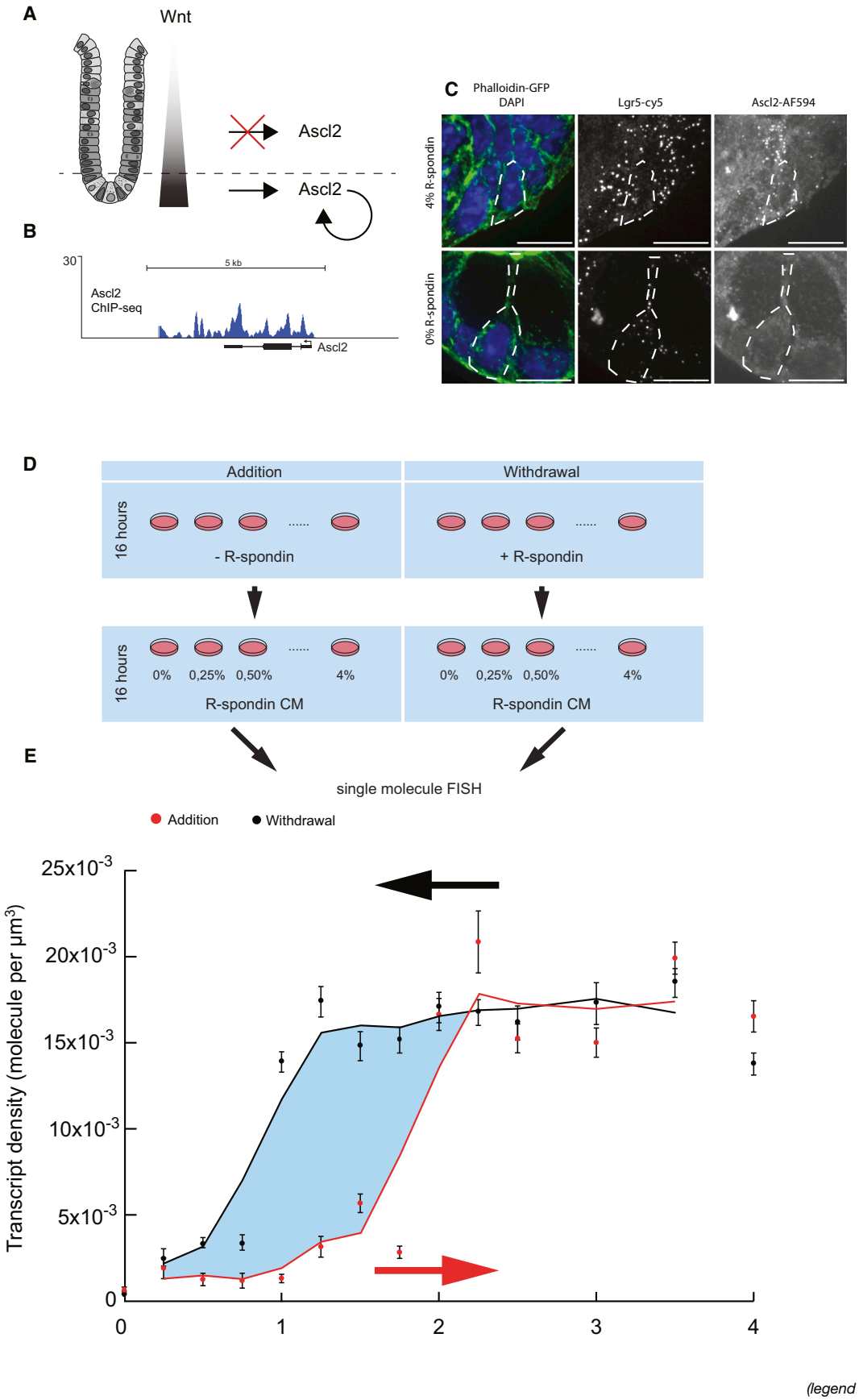

(legend on next page)

around 160 genes that are absent in TA cells (Muñoz et al., 2012). While CBC cells generate TA cells each day, TA cells can also "move" in the reverse direction to become stem cells, i.e., they exhibit plasticity within their lineage (Kim et al., 2014; Sato et al., 2011; van Es et al., 2012b).

We have previously postulated that the transcription factor Ascl2, itself encoded by a crypt-specific Wnt target gene, acts as master regulator of the crypt stem cell. When overexpressed, it induces stem cell genes and crypt neogenesis in vivo (van der Flier et al., 2009b). When deleted in vivo using the incompletely deleting AhCre transgene, the crypts are rapidly taken over by $Lgr5^+$ escaper cells. When we deleted *Ascl2* in our organoid model using the much more efficient villin-CreER transgene, mutant stem cells did not disappear but maintained a severely reduced proliferation speed. We speculate that this phenotype is apparent in the organoid culture as a result of high-efficiency induction of the Cre-recombinase, leaving no wild-type cells capable of outcompeting (Snippert et al., 2010) the $Ascl2^{-/-}$ stem cells.

In the present study, we describe how Ascl2, by controlling its own expression, is subject to an autoactivatory loop, which results in an on/off expression pattern of Ascl2. The principal driver of Ascl2 expression is the presence of Wnt/R-spondin1 signaling, but motif analysis of Ascl2 regulatory sequences yielded other candidate regulators (Table S3). The autoactivatory loop creates a Wnt/Rspondin threshold below which Ascl2 is not expressed. Indeed, when high levels of human R-spondin1 are introduced in the intestines of mice, gross hyperproliferation ensues (Kim et al., 2005). This can readily be explained by the notion that a larger number of cells in the crypts of these animals now surpass the threshold level of Wnt/R-spondin1 signaling and activate Ascl2 expression. It is interesting that Ascl2 expression depends on the previous state, i.e., the presence or absence of Wnt signals. If the cells come from a "low-Wnt-signal-strength" environment, they require stronger Wnt signals for Ascl2 activation than when they come from a "high-Wnt-signal-strength" environment. This mechanism interprets Wnt levels in crypts and translates this continuous signal into a discrete Ascl2 "on" or "off" decision. Ascl2, together with β-catenin/Tcf, activates a set of other stem cell genes (see Results; van der Flier et al., 2009b; van Es et al., 2012a). Since Ascl2 is controlled in an on/off fashion by Wnt and its autoregulatory loop, it thus constitutes a transcriptional "stemness switch" that is both Wnt responsive and Wnt dependent. One prediction from this model would be that TA cells would readily revert to a stem cell state upon increase of Wnt signal strength. Indeed, this is observed when isolated TA cells are subjected to high-level Wnt signals in culture (van Es et al., 2012b). While these precursors will not behave like stem cells to form miniguts in standard culture conditions, they will readily do so when briefly exposed to high-dose Wnt3A.

OCT4, Nanog, and *SOX2* are the regulators of pluripotency in embryonic stem cells. They act by directly occupying their target genes while collaborating in a regulatory circuitry of autoregulatory feed-forward loops to control their own as well as each other's expression (Boyer et al., 2005; Marson et al., 2008). The current mechanism only involves a single transcription factor yet is reminiscent of the way *Oct4*, *Nanog*, and *Sox2* control the stem cell phenotype of embryonic stem cells. Maintenance of the crypt stem cell phenotype hinges on the autoregulatory control of Ascl2, itself controlling stem cell genes, to impose the Lgr5 stem cell phenotype in a robust all-or-nothing fashion.

EXPERIMENTAL PROCEDURES

Crypt Isolation

Mouse intestines were flushed with PBS before being cut open longitudinally. The villi were removed by scraping with a microscope slide. Pieces of approximately 1 cm in length were incubated in 5 mM EDTA/PBS without Ca2+/Mg2+ for 15 min at 4°C per fraction. After incubation, the epithelium was separated by vigorous shaking, and the remaining intestinal tissue was placed in a new tube for collection of the following fraction. Remaining crypts were pelleted and evaluated for purity under the microscope. The two purest fractions were pooled and used as input material for ChIP-seq. All procedures were performed in compliance with local animal welfare laws, guidelines, and policies.

ChIP-seq

Primary antibodies used for immunoprecipitation (IP) are goat-anti-Tcf4 (N-20; Santa Cruz Biotechnology), rabbit-anti-β-catenin (H102; Santa Cruz), mouse-anti-Ascl2 (7E2; Millipore), and E2A (V-18; Santa Cruz). ChIP was performed as described elsewhere (Mokry et al., 2010). In brief, Ls174t cells or mouse intestinal crypts were crosslinked with 1% formaldehyde for 20 min at room temperature. For β-catenin ChIP-seq, cells were crosslinked for 40 min using ethylene glycol-bis(succinimidylsuccinate) (Thermo Scientific) at 12.5 mM final concentration, with the addition of formaldehyde (1% final concentration) after 20 min of incubation. The reaction was quenched with glycine, and the cells were successively washed with PBS, buffer B (0.25% Triton X-100, 10 mM EDTA, 0.5 mM EGTA, 20 mM HEPES, pH 7.6), and buffer C (0.15 M NaCl, 1 mM EDTA, 0.5 mM EGTA, 20 mM HEPES, pH 7.6). The cells were then resuspended in shearing buffer (0.3% SDS, 1% Triton X-100, 0.15 M NaCl, 1 mM EDTA, 0.5 mM EGTA, 20 mM HEPES, pH 7.6) and sheared using Covaris S2 (Covaris) for 8 min with the following settings: duty cycle, max; intensity, max; cycles per burst, max; mode, power tracking. The sonicated chromatin was diluted to 0.15 SDS and incubated for 12 hr at 4°C with 25 μl of the anti-TCF4 antibody, 25 μl of anti-Ascl2 antibody, or 50 μl of the anti-β-catenin antibody per IP with 100 ml protein G beads (Upstate). The beads were

Figure 6. Wnt Signaling and Ascl2 Form a Bistable Switch for Stemness

(A) Model of the Ascl2-driven feedback loop that translates in to a stable Ascl2-ON or Ascl2-OFF state, depending on the level of Wnt activation.

(B) UCSC (University of California, Santa Cruz) genome browser excerpt showing Ascl2 ChIP-seq signal over the Ascl2 locus in mouse small intestine.

(C) Fluorescence microscopy showing smFISH for *Lgr5* (Cy5) and *Ascl2* (Alexa Fluor 594) mRNA in organoid cultures. Individual dots represent single mRNA molecules. Cell membranes have been stained by GFP-coupled phalloidin, and nuclei have been stained by DAPI. Scale bars, 12.5 μm. White dashed lines indicate a single cell.

(D) Organoid cultures were cultured in the presence or absence of 5% R-spondin CM for 16 hr before the medium was changed to contain different amounts of R-spondin CM. After 16 hr, organoids were collected and processed to cryosections before being submitted to smFISH.

(E) smFISH quantification of mRNA molecules per cubic micrometer. Images were taken and cropped to contain only cells. These images were then rasterized in pseudocells with an xy area of 25 μm^2 each, and dots per pseudocell were counted. Only pseudocells that contain *Lgr5* were quantified for *Ascl2* dots. The mean transcript density (dots per cubic micrometer) was plotted. Solid lines show a sliding window average, taking the average of three adjacent data points centered on the middle of the three. Error bars indicate SEM.

See also Figure S5.

successively washed two times with buffer 1 (0.1% SDS, 0.1% deoxycholate, 1% Triton X-100, 0.15 M NaCl, 1 mM EDTA, 0.5 mM EGTA, 20 mM HEPES, pH 7.6), one time with buffer 2 (0.1% SDS, 0.1% sodium deoxycholate, 1% Triton X-100, 0.5 M NaCl, 1 mM EDTA, 0.5 mM EGTA, 20 mM HEPES, pH 7.6), one time with buffer 3 (0.25 M LiCl, 0.5% sodium deoxycholate, 0.5% NP-40, 1 mM EDTA, 0.5 mM EGTA, 20 mM HEPES, pH 7.6), and two times with buffer 4 (1 mM EDTA, 0.5 mM EGTA, 20 mM HEPES, pH 7.6) for 5 min each at 4°C. Chromatin was eluted by incubation of the beads with elution buffer (1% SDS, 0.1 M $NaHCO_3$). After washing and elution, the immunoprecipitated chromatin was decrosslinked by incubation at 65°C for 5 hr in the presence of 200 mM NaCl, extracted with phenol chloroform, and ethanol precipitated. Immunoprecipitated chromatin was additionally sheared and end repaired, sequencing adaptors were ligated, and the library was amplified by ligation-mediated PCR (LMPCR). After LMPCR, the library was purified and checked for the proper size range and for the absence of adaptor dimers on a 2% agarose gel and sequenced on a SOLiD/AB sequencer to produce reads 50 base pairs (bp) long. Sequencing reads were mapped against the reference genome. CisGenome was used for peak calling with a 0.1 false discovery rate.

To verify Ascl2 ChIP-seq, 21 randomly picked elements were confirmed in a separate ChIP-qPCR experiment (Figure S6A). As a control, ASCL2 binding was also analyzed after ASCL2 knockdown using a doxycycline-inducible small interfering RNA (siRNA) expression cassette that was stably integrated into LS174t colon cancer cells (van der Flier et al., 2009b). ASCL2 DNA occupation was significantly diminished when the siRNA was expressed (Figure S6A). Furthermore, 15 of the occupied DNA elements were tested for their capacity to act as transcriptional enhancers in a luciferase reporter gene assay. Seven of these displayed transcriptional activation upon ASCL2 cotransfection in HEK293T cells (which do not express endogenous ASCL2) (Figure S6B).

GSEA

The GSEA was performed using the freely available software from the Broad Institute, GSEAP 2.0 (http://www.broadinstitute.org/gsea/index.jsp) (Mootha et al., 2003; Subramanian et al., 2005). To create gene sets corresponding to the ChIP-seq peaks of specific TFs, individual peaks were correlated to nearest genes, and when a gene was occupied by significant TF enrichment within 5 kb of the TSS, it was incorporated in the gene set of that particular TF. The gene lists consisted of all changed or unchanged genes from the microarray analyses (no cutoff), provided that their detected signal was 2-fold above background, ranked according to the fold change. The ranked gene lists were then probed with the different gene sets with a GSEA-preranked setting. Duplicate probes were collapsed to the highest value.

Reporter Assays

Genomic fragments spanning typically about 1 kb of genomic sequence encompassing a ChiP-seq peak were amplified by PCR from human genomic DNA and cloned in front of the firefly luciferase gene in pGL4.10. In the case of TSS-proximal regions, elements were cloned directly in front of the Luciferase TSS. In the case of non-TSS-proximal regions, they were cloned in front of a minimal TATA box that was, in turn, cloned in front of the firefly luciferase gene in pGL4.10. The reporters were transfected with polyethylenimine (PEI Sigma) in all cell lines, with Renilla luciferase as a transfection control, and their activity was measured using a dual-luciferase reporter assay system (Promega). As a positive control, the previously described TOPFLASH reporter was used (Korinek et al., 1997). Empty pGL4.10 or pGL4.10TATA vectors served as negative controls. Primer sequences are listed in the Supplemental Experimental Procedures.

qPCR

For validation of ChIP-seq experiments, several peaks were confirmed using qPCR. Primers were designed using the ChIP-seq data as a reference, with amplicon sizes around 200 bp. Precipitated DNA was purified and diluted 1:20 before testing with qPCR. Reactions were performed using the SYBR-Green PCR Master Mix (Applied Biosystems) in conjumction with the BIORAD MYIQ2 qPCR machine. Obtained C(t) values were quantified using a standard made by serial dilutions of ChIP input material. Then they were normalized against the corresponding input material and, finally, against a negative control region. Primer sequences are listed in the Supplemental Experimental Procedures.

Organoid/Cell Culture

Mouse organoids were established and maintained from isolated crypts of the proximal small intestine as described elsewhere (Sato et al., 2009). The basic culture medium (advanced Dulbecco's modified Eagle's medium/F12 supplemented with penicillin/streptomycin, 10 mmol/l HEPES, 1× Glutamax, 1× B27 [all from Life Technologies], and 1 mmol/l N-acetylcysteine [Sigma]) was supplemented with 50 ng/ml murine recombinant EGF (Peprotech), R-spondin1 (CM, 5% final volume), and Noggin (CM, 10% final volume). IWP-2 was from Stemgent. CM were produced using HEK293T cells stably transfected with HA-mouse Rspo1-Fc (a gift from Calvin Kuo, Stanford University) or after transient transfection with mouse Noggin-Fc expression vector. Advanced Dulbecco's modified Eagle's medium/F12 supplemented with penicillin/streptomycin, 10 mmol/l HEPES, and 1× Glutamax was conditioned for 1 week. For complete gene deletion, 4-OHT (Sigma; 10 nmol/l) was added to the culture medium for 12 hr.

Viral Vectors

For homogeneous expression of Ascl2, the consensus cDNA was cloned into the pMSCV-loxp-dsRed-loxpeGFP-Puro-WPRE vector (available via Addgene; catalog no. 32702), and virus production, transduction, and puromycin selection were performed as described elsewhere (Koo et al., 2011).

Histology and In Situ Hybridization

Organoid cultures were fixed overnight in formalin at 4°C before paraffin embedding. In situ hybridization analysis has been described elsewhere (Gregorieff et al., 2005). For organoid sections, gentle proteinase K digestion was performed (15 ng/ml; 10 min at room temperature). The probes for Lgr5 and Olfm4 have been described previously (Tian et al., 2011; van der Flier et al., 2009a). Immunohistochemistry on organoid sections was performed as described elsewhere for intestinal sections (van Es et al., 2010); the primary antibodies used were mouse-anti-Ki67 (MM1; Monosan) and mouse-anti-Ascl2 (8F1; Millipore).

For smFISH, the organoids were harvested and washed before being fixed in BSA-coated Eppendorf microtubes in a 4% formaldehyde, 30% sucrose PBS solution overnight. The organoids were then precipitated and transferred to optimal cutting temperature compound in a mold and frozen. Then, they were sectioned and processed for smFISH as previously described (Itzkovitz et al., 2011). Individual transcript molecules were identified using previously described methods (Raj et al., 2008). All smFISH data were analyzed in Matlab using custom-written code.

Microarray Analyses

We used a previously described microarray analysis of sorted $Lgr5^+$ cells isolated from Lgr5GFP-IRES-CreERT mice (Muñoz et al., 2012). Intestinal organoids of different genotypes, maintaining or missing *Tcf7l2*, overexpressing or with endogenous levels of Ascl2, were harvested by adding 350 μl of Buffer RLT containing β-mercaptoethanol directly to the Matrigel (Corning Life Sciences). RNA was purified using the QIAGEN RNeasy Mini Kit and then prepared for microarray hybridization according to the Agilent protocol. Labeled cRNA was hybridized on the Agilent 4x44k Whole Mouse Genome Microarray Kit.

Motif Analysis

One kilobase and the whole annotated 5′ untranslated region of mouse and human Ascl2 were analyzed for motif presence using ConTrav2 software, with parameters set to 90% of core motif and 75% of position weight matrix match rate cutoff.

ACCESSION NUMBERS

The data sets used in this study that have not been published elsewhere are deposited in Gene Expression Omnibus and are available with accession number GSE57053.

SUPPLEMENTAL INFORMATION

Supplemental Information includes six figures, and three tables, and Supplemental Experimental Procedures and can be found with this article online at http://dx.doi.org/10.1016/j.stem.2014.12.006.

AUTHOR CONTRIBUTIONS

J.S. performed experimental procedures under the guidance of H.C. J.S. and H.C. wrote the manuscript. J.J. and J.S. analyzed the smFISH data that were generated with the help of V.S. under the guidance of A.v.O. M.M. and J.S. analyzed the ChIP-seq data that were generated with P.H. and sequenced under the guidance of E.C. L.v.d.F. generated the Ascl2-loxp animal model. B.K. and J.S. performed viral transductions of organoid cultures.

ACKNOWLEDGMENTS

The authors thank Marc van de Wetering and Wim de Lau for helpful discussions and Anna Lyubimova for sharing her expertise on smFISH.

Received: June 2, 2014
Revised: November 18, 2014
Accepted: December 17, 2014
Published: January 22, 2015

REFERENCES

Acar, M., Mettetal, J.T., and van Oudenaarden, A. (2008). Stochastic switching as a survival strategy in fluctuating environments. Nat. Genet. *40*, 471–475.

Andreu, P., Colnot, S., Godard, C., Gad, S., Chafey, P., Niwa-Kawakita, M., Laurent-Puig, P., Kahn, A., Robine, S., Perret, C., and Romagnolo, B. (2005). Crypt-restricted proliferation and commitment to the Paneth cell lineage following Apc loss in the mouse intestine. Development *132*, 1443–1451.

Andreu, P., Peignon, G., Slomianny, C., Taketo, M.M., Colnot, S., Robine, S., Lamarque, D., Laurent-Puig, P., Perret, C., and Romagnolo, B. (2008). A genetic study of the role of the Wnt/beta-catenin signalling in Paneth cell differentiation. Dev. Biol. *324*, 288–296.

Barker, N., van Es, J.H., Kuipers, J., Kujala, P., van den Born, M., Cozijnsen, M., Haegebarth, A., Korving, J., Begthel, H., Peters, P.J., and Clevers, H. (2007). Identification of stem cells in small intestine and colon by marker gene Lgr5. Nature *449*, 1003–1007.

Batlle, E., Henderson, J.T., Beghtel, H., van den Born, M.M., Sancho, E., Huls, G., Meeldijk, J., Robertson, J., van de Wetering, M., Pawson, T., and Clevers, H. (2002). Beta-catenin and TCF mediate cell positioning in the intestinal epithelium by controlling the expression of EphB/ephrinB. Cell *111*, 251–263.

Bevins, C.L., and Salzman, N.H. (2011). Paneth cells, antimicrobial peptides and maintenance of intestinal homeostasis. Nat. Rev. Microbiol. *9*, 356–368.

Bjerknes, M., and Cheng, H. (1981). The stem-cell zone of the small intestinal epithelium. I. Evidence from Paneth cells in the adult mouse. Am. J. Anat. *160*, 51–63.

Boyer, L.A., Lee, T.I., Cole, M.F., Johnstone, S.E., Levine, S.S., Zucker, J.P., Guenther, M.G., Kumar, R.M., Murray, H.L., Jenner, R.G., et al. (2005). Core transcriptional regulatory circuitry in human embryonic stem cells. Cell *122*, 947–956.

Carmon, K.S., Gong, X., Lin, Q., Thomas, A., and Liu, Q. (2011). R-spondins function as ligands of the orphan receptors LGR4 and LGR5 to regulate Wnt/beta-catenin signaling. Proc. Natl. Acad. Sci. USA *108*, 11452–11457.

Cheng, H., and Leblond, C.P. (1974). Origin, differentiation and renewal of the four main epithelial cell types in the mouse small intestine. I. Columnar cell. Am. J. Anat. *141*, 461–479.

Clevers, H. (2013). The intestinal crypt, a prototype stem cell compartment. Cell *154*, 274–284.

Davies, P.S., Dismuke, A.D., Powell, A.E., Carroll, K.H., and Wong, M.H. (2008). Wnt-reporter expression pattern in the mouse intestine during homeostasis. BMC Gastroenterol. *8*, 57.

de Lau, W., Barker, N., Low, T.Y., Koo, B.K., Li, V.S., Teunissen, H., Kujala, P., Haegebarth, A., Peters, P.J., van de Wetering, M., et al. (2011). Lgr5 homologues associate with Wnt receptors and mediate R-spondin signalling. Nature *476*, 293–297.

de Sousa E Melo, F., Colak, S., Buikhuisen, J., Koster, J., Cameron, K., de Jong, J.H., Tuynman, J.B., Prasetyanti, P.R., Fessler, E., van den Bergh, S.P., et al. (2011). Methylation of cancer-stem-cell-associated Wnt target genes predicts poor prognosis in colorectal cancer patients. Cell Stem Cell *9*, 476–485.

Farin, H.F., Van Es, J.H., and Clevers, H. (2012).). Redundant sources of Wnt regulate intestinal stem cells and promote formation of Paneth cells. Gastroenterology *143*, 1518–1529, e1517.

Fevr, T., Robine, S., Louvard, D., and Huelsken, J. (2007). Wnt/beta-catenin is essential for intestinal homeostasis and maintenance of intestinal stem cells. Mol. Cell. Biol. *27*, 7551–7559.

Glinka, A., Dolde, C., Kirsch, N., Huang, Y.L., Kazanskaya, O., Ingelfinger, D., Boutros, M., Cruciat, C.M., and Niehrs, C. (2011). LGR4 and LGR5 are R-spondin receptors mediating Wnt/β-catenin and Wnt/PCP signalling. EMBO Rep. *12*, 1055–1061.

Gregorieff, A., Pinto, D., Begthel, H., Destrée, O., Kielman, M., and Clevers, H. (2005). Expression pattern of Wnt signaling components in the adult intestine. Gastroenterology *129*, 626–638.

Guillemot, F., Nagy, A., Auerbach, A., Rossant, J., and Joyner, A.L. (1994). Essential role of Mash-2 in extraembryonic development. Nature *371*, 333–336.

Hao, H.X., Xie, Y., Zhang, Y., Charlat, O., Oster, E., Avello, M., Lei, H., Mickanin, C., Liu, D., Ruffner, H., et al. (2012). ZNRF3 promotes Wnt receptor turnover in an R-spondin-sensitive manner. Nature *485*, 195–200.

Haramis, A.P., Begthel, H., van den Born, M., van Es, J., Jonkheer, S., Offerhaus, G.J., and Clevers, H. (2004). De novo crypt formation and juvenile polyposis on BMP inhibition in mouse intestine. Science *303*, 1684–1686.

Hatzis, P., van der Flier, L.G., van Driel, M.A., Guryev, V., Nielsen, F., Denissov, S., Nijman, I.J., Koster, J., Santo, E.E., Welboren, W., et al. (2008). Genome-wide pattern of TCF7L2/TCF4 chromatin occupancy in colorectal cancer cells. Mol. Cell. Biol. *28*, 2732–2744.

Hirata, A., Utikal, J., Yamashita, S., Aoki, H., Watanabe, A., Yamamoto, T., Okano, H., Bardeesy, N., Kunisada, T., Ushijima, T., et al. (2013). Dose-dependent roles for canonical Wnt signalling in de novo crypt formation and cell cycle properties of the colonic epithelium. Development *140*, 66–75.

Ireland, H., Kemp, R., Houghton, C., Howard, L., Clarke, A.R., Sansom, O.J., and Winton, D.J. (2004). Inducible Cre-mediated control of gene expression in the murine gastrointestinal tract: effect of loss of beta-catenin. Gastroenterology *126*, 1236–1246.

Itzkovitz, S., Lyubimova, A., Blat, I.C., Maynard, M., van Es, J., Lees, J., Jacks, T., Clevers, H., and van Oudenaarden, A. (2011). Single-molecule transcript counting of stem-cell markers in the mouse intestine. Nat. Cell Biol. *14*, 106–114.

Johnson, J.E., Birren, S.J., and Anderson, D.J. (1990). Two rat homologues of Drosophila achaete-scute specifically expressed in neuronal precursors. Nature *346*, 858–861.

Jubb, A.M., Chalasani, S., Frantz, G.D., Smits, R., Grabsch, H.I., Kavi, V., Maughan, N.J., Hillan, K.J., Quirke, P., and Koeppen, H. (2006). Achaete-scute like 2 (ascl2) is a target of Wnt signalling and is upregulated in intestinal neoplasia. Oncogene *25*, 3445–3457.

Jung, P., Sato, T., Merlos-Suárez, A., Barriga, F.M., Iglesias, M., Rossell, D., Auer, H., Gallardo, M., Blasco, M.A., Sancho, E., et al. (2011). Isolation and in vitro expansion of human colonic stem cells. Nat. Med. *17*, 1225–1227.

Kabiri, Z., Greicius, G., Madan, B., Biechele, S., Zhong, Z., Zaribafzadeh, H., Edison, Aliyev, J., Wu, Y., Bunte, R., et al. (2014). Stroma provides an intestinal stem cell niche in the absence of epithelial Wnts. Development *141*, 2206–2215.

Kim, K.A., Kakitani, M., Zhao, J., Oshima, T., Tang, T., Binnerts, M., Liu, Y., Boyle, B., Park, E., Emtage, P., et al. (2005). Mitogenic influence of human R-spondin1 on the intestinal epithelium. Science *309*, 1256–1259.

Kim, T.H., Li, F., Ferreiro-Neira, I., Ho, L.L., Luyten, A., Nalapareddy, K., Long, H., Verzi, M., and Shivdasani, R.A. (2014). Broadly permissive intestinal chromatin underlies lateral inhibition and cell plasticity. Nature *506*, 511–515.

Koo, B.K., Stange, D.E., Sato, T., Karthaus, W., Farin, H.F., Huch, M., van Es, J.H., and Clevers, H. (2011). Controlled gene expression in primary Lgr5 organoid cultures. Nat. Methods *9*, 81–83.

Koo, B.K., Spit, M., Jordens, I., Low, T.Y., Stange, D.E., van de Wetering, M., van Es, J.H., Mohammed, S., Heck, A.J., Maurice, M.M., and Clevers, H. (2012). Tumour suppressor RNF43 is a stem-cell E3 ligase that induces endocytosis of Wnt receptors. Nature *488*, 665–669.

Korinek, V., Barker, N., Morin, P.J., van Wichen, D., de Weger, R., Kinzler, K.W., Vogelstein, B., and Clevers, H. (1997). Constitutive transcriptional activation by a beta-catenin-Tcf complex in APC-/- colon carcinoma. Science *275*, 1784–1787.

Korinek, V., Barker, N., Moerer, P., van Donselaar, E., Huls, G., Peters, P.J., and Clevers, H. (1998). Depletion of epithelial stem-cell compartments in the small intestine of mice lacking Tcf-4. Nat. Genet. *19*, 379–383.

Kuhnert, F., Davis, C.R., Wang, H.T., Chu, P., Lee, M., Yuan, J., Nusse, R., and Kuo, C.J. (2004). Essential requirement for Wnt signaling in proliferation of adult small intestine and colon revealed by adenoviral expression of Dickkopf-1. Proc. Natl. Acad. Sci. USA *101*, 266–271.

Liu, X., Chen, X., Zhong, B., Wang, A., Wang, X., Chu, F., Nurieva, R.I., Yan, X., Chen, P., van der Flier, L.G., et al. (2014). Transcription factor achaete-scute homologue 2 initiates follicular T-helper-cell development. Nature *507*, 513–518.

Marson, A., Levine, S.S., Cole, M.F., Frampton, G.M., Brambrink, T., Johnstone, S., Guenther, M.G., Johnston, W.K., Wernig, M., Newman, J., et al. (2008). Connecting microRNA genes to the core transcriptional regulatory circuitry of embryonic stem cells. Cell *134*, 521–533.

Mokry, M., Hatzis, P., de Bruijn, E., Koster, J., Versteeg, R., Schuijers, J., van de Wetering, M., Guryev, V., Clevers, H., and Cuppen, E. (2010). Efficient double fragmentation ChIP-seq provides nucleotide resolution protein-DNA binding profiles. PLoS ONE *5*, e15092.

Mootha, V.K., Lindgren, C.M., Eriksson, K.F., Subramanian, A., Sihag, S., Lehar, J., Puigserver, P., Carlsson, E., Ridderstråle, M., Laurila, E., et al. (2003). PGC-1alpha-responsive genes involved in oxidative phosphorylation are coordinately downregulated in human diabetes. Nat. Genet. *34*, 267–273.

Morin, P.J., Sparks, A.B., Korinek, V., Barker, N., Clevers, H., Vogelstein, B., and Kinzler, K.W. (1997). Activation of beta-catenin-Tcf signaling in colon cancer by mutations in beta-catenin or APC. Science *275*, 1787–1790.

Muñoz, J., Stange, D.E., Schepers, A.G., van de Wetering, M., Koo, B.K., Itzkovitz, S., Volckmann, R., Kung, K.S., Koster, J., Radulescu, S., et al. (2012). The Lgr5 intestinal stem cell signature: robust expression of proposed quiescent '+4' cell markers. EMBO J. *31*, 3079–3091.

Ogawa, H., Ishiguro, K., Gaubatz, S., Livingston, D.M., and Nakatani, Y. (2002). A complex with chromatin modifiers that occupies E2F- and Myc-responsive genes in G0 cells. Science *296*, 1132–1136.

Ozbudak, E.M., Thattai, M., Lim, H.N., Shraiman, B.I., and Van Oudenaarden, A. (2004). Multistability in the lactose utilization network of Escherichia coli. Nature *427*, 737–740.

Pinto, D., Robine, S., Jaisser, F., El Marjou, F.E., and Louvard, D. (1999). Regulatory sequences of the mouse villin gene that efficiently drive transgenic expression in immature and differentiated epithelial cells of small and large intestines. J. Biol. Chem. *274*, 6476–6482.

Pinto, D., Gregorieff, A., Begthel, H., and Clevers, H. (2003). Canonical Wnt signals are essential for homeostasis of the intestinal epithelium. Genes Dev. *17*, 1709–1713.

Polakis, P. (1999). The oncogenic activation of beta-catenin. Curr. Opin. Genet. Dev. *9*, 15–21.

Raj, A., van den Bogaard, P., Rifkin, S.A., van Oudenaarden, A., and Tyagi, S. (2008). Imaging individual mRNA molecules using multiple singly labeled probes. Nat. Methods *5*, 877–879.

Reed, K.R., Tunster, S.J., Young, M., Carrico, A., John, R.M., and Clarke, A.R. (2012). Entopic overexpression of Ascl2 does not accelerate tumourigenesis in ApcMin mice. Gut *61*, 1435–1438.

San Roman, A.K., Jayewickreme, C.D., Murtaugh, L.C., and Shivdasani, R.A. (2014). Wnt secretion from epithelial cells and subepithelial myofibroblasts is not required in the mouse intestinal stem cell niche in vivo. Stem Cell Reports *2*, 127–134.

Sansom, O.J., Reed, K.R., Hayes, A.J., Ireland, H., Brinkmann, H., Newton, I.P., Batlle, E., Simon-Assmann, P., Clevers, H., Nathke, I.S., et al. (2004). Loss of Apc in vivo immediately perturbs Wnt signaling, differentiation, and migration. Genes Dev. *18*, 1385–1390.

Sato, T., Vries, R.G., Snippert, H.J., van de Wetering, M., Barker, N., Stange, D.E., van Es, J.H., Abo, A., Kujala, P., Peters, P.J., and Clevers, H. (2009). Single Lgr5 stem cells build crypt-villus structures in vitro without a mesenchymal niche. Nature *459*, 262–265.

Sato, T., van Es, J.H., Snippert, H.J., Stange, D.E., Vries, R.G., van den Born, M., Barker, N., Shroyer, N.F., van de Wetering, M., and Clevers, H. (2011). Paneth cells constitute the niche for Lgr5 stem cells in intestinal crypts. Nature *469*, 415–418.

Schuijers, J., Mokry, M., Hatzis, P., Cuppen, E., and Clevers, H. (2014). Wnt-induced transcriptional activation is exclusively mediated by TCF/LEF. EMBO J. *33*, 146–156.

Snippert, H.J., van der Flier, L.G., Sato, T., van Es, J.H., van den Born, M., Kroon-Veenboer, C., Barker, N., Klein, A.M., van Rheenen, J., Simons, B.D., and Clevers, H. (2010). Intestinal crypt homeostasis results from neutral competition between symmetrically dividing Lgr5 stem cells. Cell *143*, 134–144.

Stevens, C.E., and Leblond, C.P. (1947). Rate of renewal of the cells of the intestinal epithelium in the rat. Anat. Rec. *97*, 373.

Subramanian, A., Tamayo, P., Mootha, V.K., Mukherjee, S., Ebert, B.L., Gillette, M.A., Paulovich, A., Pomeroy, S.L., Golub, T.R., Lander, E.S., and Mesirov, J.P. (2005). Gene set enrichment analysis: a knowledge-based approach for interpreting genome-wide expression profiles. Proc. Natl. Acad. Sci. USA *102*, 15545–15550.

ten Kate, J., Eidelman, S., Bosman, F.T., and Damjanov, I. (1989). Expression of c-myc proto-oncogene in normal human intestinal epithelium. J. Histochem. Cytochem. *37*, 541–545.

Tian, H., Biehs, B., Warming, S., Leong, K.G., Rangell, L., Klein, O.D., and de Sauvage, F.J. (2011). A reserve stem cell population in small intestine renders Lgr5-positive cells dispensable. Nature *478*, 255–259.

van de Wetering, M., Cavallo, R., Dooijes, D., van Beest, M., van Es, J., Loureiro, J., Ypma, A., Hursh, D., Jones, T., Bejsovec, A., et al. (1997). Armadillo coactivates transcription driven by the product of the Drosophila segment polarity gene dTCF. Cell *88*, 789–799.

Van der Flier, L.G., Sabates-Bellver, J., Oving, I., Haegebarth, A., De Palo, M., Anti, M., Van Gijn, M.E., Suijkerbuijk, S., Van de Wetering, M., Marra, G., and Clevers, H. (2007). The intestinal Wnt/TCF signature. Gastroenterology *132*, 628–632.

van der Flier, L.G., Haegebarth, A., Stange, D.E., van de Wetering, M., and Clevers, H. (2009a). OLFM4 is a robust marker for stem cells in human intestine and marks a subset of colorectal cancer cells. Gastroenterology *137*, 15–17.

van der Flier, L.G., van Gijn, M.E., Hatzis, P., Kujala, P., Haegebarth, A., Stange, D.E., Begthel, H., van den Born, M., Guryev, V., Oving, I., et al. (2009b). Transcription factor achaete scute-like 2 controls intestinal stem cell fate. Cell *136*, 903–912.

van Es, J.H., Jay, P., Gregorieff, A., van Gijn, M.E., Jonkheer, S., Hatzis, P., Thiele, A., van den Born, M., Begthel, H., Brabletz, T., et al. (2005a). Wnt signalling induces maturation of Paneth cells in intestinal crypts. Nat. Cell Biol. *7*, 381–386.

van Es, J.H., van Gijn, M.E., Riccio, O., van den Born, M., Vooijs, M., Begthel, H., Cozijnsen, M., Robine, S., Winton, D.J., Radtke, F., and Clevers, H. (2005b). Notch/gamma-secretase inhibition turns proliferative cells in intestinal crypts and adenomas into goblet cells. Nature *435*, 959–963.

van Es, J.H., de Geest, N., van de Born, M., Clevers, H., and Hassan, B.A. (2010). Intestinal stem cells lacking the Math1 tumour suppressor are refractory to Notch inhibitors. Nat. Commun. *1*, 18.

van Es, J.H., Haegebarth, A., Kujala, P., Itzkovitz, S., Koo, B.K., Boj, S.F., Korving, J., van den Born, M., van Oudenaarden, A., Robine, S., and Clevers, H. (2012a). A critical role for the Wnt effector Tcf4 in adult intestinal homeostatic self-renewal. Mol. Cell. Biol. *32*, 1918–1927.

van Es, J.H., Sato, T., van de Wetering, M., Lyubimova, A., Nee, A.N., Gregorieff, A., Sasaki, N., Zeinstra, L., van den Born, M., Korving, J., et al. (2012b). Dll1+ secretory progenitor cells revert to stem cells upon crypt damage. Nat. Cell Biol. *14*, 1099–1104.

Wu, C., Qiu, S., Lu, L., Zou, J., Li, W.F., Wang, O., Zhao, H., Wang, H., Tang, J., Chen, L., et al. (2014). RSPO2-LGR5 signaling has tumour-suppressive activity in colorectal cancer. Nat. Commun. *5*, 3149.

Xiong, W., and Ferrell, J.E., Jr. (2003). A positive-feedback-based bistable 'memory module' that governs a cell fate decision. Nature *426*, 460–465.

Yin, X., Farin, H.F., van Es, J.H., Clevers, H., Langer, R., and Karp, J.M. (2014). Niche-independent high-purity cultures of Lgr5+ intestinal stem cells and their progeny. Nat. Methods *11*, 106–112.